Redox Biology 28 (2020) 101327

Contents lists available at ScienceDirect

Redox Biology

journal homepage: www.elsevier.com/locate/redox

Research Paper

Insufficiency of melatonin in follicular fluid is a reversible cause for advanced maternal age-related aneuploidy in oocytes

Mianqun Zhang[1], Yajuan Lu[1], Ying Chen[1], Yu Zhang, Bo Xiong*

College of Animal Science and Technology, Nanjing Agricultural University, Nanjing, 210095, China

ARTICLE INFO

Keywords:
Oocyte quality
Melatonin
Follicular fluid
Reactive oxygen species
Aneuploidy

ABSTRACT

Age-related decline in female fertility is a common feature that occurs in the fourth decade of women as a result of a reduction in both oocyte quality and quantity [1]. However, strategies to prevent the deterioration of maternal aged oocytes and relevant mechanisms are still underexplored. Here, we find that the reduced abundance of melatonin in the follicular fluid highly correlates with the advanced maternal age-related aneuploidy. Of note, we show that exposure of oocytes from aged mice both *in vitro* and *in vivo* to exogenous melatonin not only eliminates the accumulated reactive oxygen species-induced DNA damage and apoptosis, but also suppresses the occurrence of aneuploidy caused by spindle/chromosome defect that is frequently observed in aged oocytes. Importantly, we reveal that melatonin supplementation reverses the defective phenotypes in aged oocytes through a Sirt1/Sod2-dependent mechanism. Inhibition of Sirt1 activity abolishes the melatonin-mediated improvement of aged oocyte quality. Together our findings provide evidence that supplementation of melatonin is a feasible way to protect oocytes from advanced maternal age-related meiotic defects and aneuploidy, demonstrating the potential for improving the quality of oocytes from aged women and the efficiency of assisted reproductive technology.

1. Introduction

Fertility in women starts declining at age 35 years and decreases more rapidly after age 40 years [1–4], with a dramatically increased incidence of infertility, miscarriage, congenital birth defects and fetal aneuploidy [5,6]. Accumulating evidence has indicated that poor oocyte quality is a common and unmanageable problem for women with advanced maternal age, which leads to the unsuccessful reproductive outcome [7–9]. Age-related quality decrease in the ovary reserve occurs as a result of two processes: increased oxidative damage in oocytes caused by excessive reactive oxygen species (ROS) [10–12] and compromised antioxidant defense systems. ROS is produced primarily in the mitochondria as a byproduct of metabolism. ROS levels exceeding the antioxidant scavenging capacity will result in DNA damage, cell cycle arrest, cellular dysfunction and apoptosis [13,14]. Thus, the balance between the production and scavenging of ROS establishes redox homeostasis and is essential for the quality of oocytes.

Melatonin is a natural hormone primarily secreted by the pineal gland which regulates the circadian rhythms [15,16]. In the meantime, as a robust antioxidant, melatonin readily scavenges the most toxic free radicals to prevent the deterioration of cells [17]. Notably, melatonin exists in the follicular fluid produced by the ovarian and granulosa cells in addition to possibly taking it up from the blood [18]. Therefore, melatonin plays an important role in the regulation of follicle development and ovarian function in different mammalian species [19–21]. The melatonin level in human follicular fluid highly correlates with the ovarian reserve and *in vitro* fertilization outcomes [21,22]. However, the relationship between the endogenous level of melatonin and advanced maternal age-related decline of oocyte quality remains elusive.

In the present study, we discovered that maternal aging-induced loss of melatonin in follicular fluid resulted in the accumulation of excessive ROS in oocytes, which leads to meiotic failure and occurrence of aneuploid eggs. Supplementation of melatonin both *in vitro* and *in vivo* ameliorated the oocyte quality through activation of the Sirt1/Sod2 pathway.

2. Materials and methods

2.1. Animals

All mice were handled in accordance with the Animal Research Institute Committee guidelines of Nanjing Agricultural University,

* Corresponding author. College of Animal Science and Technology, Nanjing Agricultural University, Nanjing, China.
E-mail address: xiongbo@njau.edu.cn (B. Xiong).
[1] These authors contributed equally to this work.

https://doi.org/10.1016/j.redox.2019.101327
Received 9 July 2019; Received in revised form 7 September 2019; Accepted 11 September 2019
Available online 12 September 2019

China. The young (6~8-week-old) and aged (44–48-week-old) C57BL/6 female mice were kept at controlled condition of temperature (20–23°C) and illumination (12 h light-dark cycle), and had free access to food and water throughout the period of the study. During the collection of oocytes, mice were treated humanely and with regard for alleviation of suffering.

2.2. Antibodies

Rabbit polyclonal anti-human γH2AX antibody and rabbit monoclonal anti-Gapdh antibody were purchased from Cell Signaling Technology (Danvers, MA, USA). Mouse monoclonal anti-α-tubulin-FITC was purchased from Sigma (St. Louis, MO, USA). Human anti-centromere antibody was purchased from Antibodies Incorporated (Davis, CA, USA). Rabbit polyclonal anti-Sirt1 antibody and rabbit polyclonal anti-Sod2 antibody were purchased from Proteintech (Rosemont, IL, USA). Alexa Fluor 488-conjugated goat anti-rabbit IgG (H + L), Alexa Fluor 555-conjugated goat anti-human IgG (H + L) were purchased from ThermoFisher (Waltham, MA, USA). HRP-conjugated goat anti-rabbit IgG (H + L) were purchased from Abcam (Cambridge, MA, USA).

2.3. Measurement of melatonin concentrations in the blood serum and follicular fluid

The samples of blood serum and follicular fluid in all groups were collected at the same time at 10 pm of the day. The concentrations of melatonin in blood serum and follicular fluid were determined by a competitive binding ELISA using the mouse melatonin ELISA kit (Kit RGB& CHN, Beijing, China). Briefly, samples or standards were added to wells coated with a goat anti-mouse IgG antibody. A monoclonal antibody specific to melatonin and a solution of a biotin labeled melatonin tracer were added to the wells. The antibody bound to melatonin in the sample or to the tracer in a competitive manner. The plate was washed, leaving only bound melatonin and bound tracer on the plate. Then, a solution of Horseradish Peroxidase conjugated Streptavidin (Strep-HRP) was added, which bound to the biotinylated tracer. After incubation, excessive Strep-HRP was washed out and TMB (tetramethylbenzidine) substrate solution was added and incubated. An HRP-catalyzed reaction generated a blue color in the solution. Stop solution was added to stop the substrate reaction. The resulting yellow color was read at 450 nm. The amount of signal was inversely proportional to the level of melatonin in the sample.

2.4. Treatment of melatonin and luzindole

For *in vitro* treatment, melatonin (Sigma) was dissolved in the absolute ethanol and diluted with maturation medium to a final concentration of 10 μM. Luzindole (Sigma) was dissolved in DMSO and diluted with maturation medium to a final concentration of 1 μM. Melatonin and/or luzindole were supplemented to the maturation medium at the beginning of culture, followed by 8 h of culture to metaphase I stage and 12 h of culture to metaphase II stage. For *in vivo* treatment, female mice were intravenously administered with 100 mg/kg body weight of melatonin and/or 10 mg/kg body weight of luzindole at 8 pm of the day for 10 days preceding oocyte collection and analysis. PBS was administered as the vehicle group.

2.5. Oocyte collection and culture

Female mice were sacrificed by cervical dislocation. Fully-grown oocytes arrested at prophase of meiosis I were collected from ovaries in M2 medium. Only those immature oocytes displaying a germinal vesicle (GV) were cultured further in M16 medium under liquid paraffin oil at 37°C in an atmosphere of 5% CO2 incubator for *in vitro* maturation. At different time points after culture (8 h for metaphase I stage and 12 h for metaphase II stage), oocytes were collected for subsequent analysis.

2.6. Determination of ROS generation

For MitoSOX staining, GV oocytes were incubated in M2 media containing 5 μM MitoSOX Red (ThermoFisher, Waltham, MA, USA) in a dark, humidified atmosphere for 10 min at 37°C. After washing three times in DPBS containing 0.1% BSA under low light, oocytes were imaged under a confocal microscope (Carl Zeiss 700).

For DCFH staining, GV oocytes were incubated with the oxidation-sensitive fluorescent probe [dichlorofluorescein (DCFH)] for 30 min at 37°C in DPBS that contained 10 μM DCFH diacetate (DCFHDA) (Beyotime Institute of Biotechnology, Hangzhou, China). Then oocytes were washed three times in DPBS containing 0.1% BSA and placed on glass slides and observed under a confocal microscope. Fluorescent signals were acquired by the confocal microscope with the same scanning settings.

2.7. Annexin-V staining

According to the manufacturer's instruction (Beyotime Institute of Biotechnology, Hangzhou, China), mouse oocytes at GV stage were stained with the Annexin-V staining kit. After washing twice in PBS, the viable oocytes were stained with 90 μl of binding buffer containing 10 μl of Annexin-V-FITC for 30 min in the dark. Fluorescent signals were acquired by the confocal microscope with the same scanning settings (Zeiss LSM 700 META).

2.8. Immunofluorescence and confocal microscopy

Oocytes were fixed in 4% paraformaldehyde in PBS (pH 7.4) for 30 min and permeabilized in 0.5% Triton-X-100 for 20 min at room temperature. Then, oocytes were blocked with 1% BSA-supplemented PBS for 1 h and incubated with anti-γH2AX (1:100), anti-α-tubulin-FITC (1:300) or anti-centromere (1:200) antibodies at 4°C overnight. After washing four times (5 min each) in PBS containing 1% Tween 20 and 0.01% Triton-X 100, oocytes were incubated with an appropriate secondary antibody for 1 h at room temperature. Then oocytes were counterstained with PI or Hoechst for 10 min. Finally, oocytes were mounted on glass slides and observed under a confocal microscope (Carl Zeiss 700).

For measurement of fluorescence intensity, the signals from different groups of oocytes were acquired by performing the same immunostaining procedure and setting up the same parameters of confocal microscope. The average fluorescence intensity per unit area within the region of interest (ROI) was applied to quantify the fluorescence of each oocyte images. Fluorescence intensity was randomly measured by plot profiling using ImageJ software (NIH, USA).

2.9. Western blotting analysis

Oocytes at GV stage were lysed in 4 × LDS sample buffer (ThermoFisher, Waltham, MA, USA) containing protease inhibitor, and then separated on 10% Bis-Tris precast gels and transferred onto PVDF membranes. The blots were blocked in TBST containing 5% low fat dry milk for 1 h at room temperature and then incubated with anti-Sirt1 (1:1000), anti-Sod2 (1:1000) or anti-Gapdh (1:5000) antibodies overnight at 4°C. After wash in TBST, the blots were incubated with HRP conjugated secondary antibodies for 1 h at room temperature. Chemiluminescence was detected with ECL Plus (GE, Piscataway, NJ, USA) and protein bands were acquired by Tanon-3900 Chemiluminescence Imaging System.

2.10. RNA-seq

Oocytes at GV stage were collected from young, aged and

melatonin-rescued mice (100 oocytes per group), respectively, and then directly lysed with 4 μl lysis buffer (0.2% Triton X-100, RNase inhibitor, dNTPs, oligo-dT primers and 100 pg mCherry mRNA spike in). Total RNA was extracted from each group using the RNeasy Plus Micro kit (Qiagen) following the manufacturer's protocol. Before RNA isolation, 2×10^6 mRNA-RFP was added to calculate mRNA copy number in each sample. Extracted total RNA was used to build a sequencing library using the NEB Next Ultra RNA Library Prep Kit for Illumina. We sequenced the library by Illumina Hiseq 2500 and aligned RNA-seq reads to *Mus musculus* UCSC mm9 references with the Tophat software (http://tophat.cbcb.umd.edu/), and calculated the FPKM of each gene using Cufflinks (http://cufflinks.cbcb.umd.edu). The amount of total mRNA was calculated based on the FPKM of exogenous RFP.

2.11. Quantitative real time PCR (qRT-PCR)

A total of 50 GV oocytes in control, aging and melatonin-administered groups were collected, respectively. Total RNA was extracted from the oocytes using RNeasy Mini Kit (Qiagen, MD, USA), and then it was reversed to cDNA and stored at -20°C until use. Each PCR reaction consisted of 10 μL of Advanced SYBR Green PCR Master Mix, 4.8 μL of water, 4 μL of cDNA sample, and 1.2 μL of gene-specific primers. Gene expression was determined by quantitative RT-PCR using a One Step SYBR PrimeScript RT-PCR Kit (TaKaRa, Tokyo, Japan) in a Light Cycler instrument (Roche, Mannheim, Germany). Experiments were performed at least three times.

2.12. Statistical analysis

The data were expressed as mean ± SEM or mean ± SD and analyzed by one-way ANOVA, followed by LSD's post hoc test, which was provided by SPSS16.0 statistical software. The level of significance was accepted as $p < 0.05$.

3. Results

3.1. Maternal aging causes the reduction of melatonin in follicular fluid and accumulation of ROS in oocytes

To determine the correlation between maternal aging and melatonin levels *in vivo*, we collected blood serum and follicular fluid from young and aged mice, respectively. We found that melatonin levels in both blood serum and follicular fluid from aged mice were remarkably lower than those from young mice (Figs. S1A and B), indicating that the abundance of endogenous melatonin decreases with age. Notably, the overall melatonin level remained higher in follicular fluid than in blood serum (Figs. S1A and B), which suggests that the maintenance of high melatonin concentration in the follicular fluid microenvironment is crucial for female ovary development and oocyte quality.

We proposed that reduction of endogenous melatonin level in follicular fluid would induce an imbalance of ROS in oocytes. To test this, ROS levels were measured using both MitoSOX and DCFH staining. The imaging data showed that ROS signals were apparently up-regulated in varying degrees in the aged oocytes as compared with the young oocytes (Figs. S2A and C), which was corroborated by the quantitative analysis of fluorescence intensity (Figs. S2B and D). In the meantime, maternal aging also prominently increased the signals of γH2AX foci in the germinal vesicle of oocytes, which is indicative of accumulated DNA damage (Figs. S3A and B). Consequently, the incidence of apoptosis was much frequently observed in aged oocytes as assessed by Annexin-V staining to detect the translocation of phosphatidylserine from the inner to the outer leaflet of the oocyte membrane, which is indicative of early apoptosis (Figs. S4A and B). Taken together, these observations suggest that apoptosis occurs in aged oocytes, which might be caused by the excessive accumulation of ROS and DNA damage.

3.2. Maternal aging induces meiotic defects and aneuploidy in oocytes

Given that excessive ROS production usually influences oocyte quality, we assessed the meiotic progression by recording the occurrence of germinal vesicle breakdown (GVBD) and first polar body extrusion (PBE) in aged oocytes. The quantitative data showed that no distinguishable differences in GVBD rate between the young and aged mice (Fig. S5A). However, at 6 and 7 h post-GVBD, the proportion of PBE was significantly higher in the aged oocytes than in the young oocytes (Figs. S5B and C), which suggests that meiotic progression was accelerated during oocyte maturation in the aged mice. Additionally, at 9 and 10 h post-GVBD, the incidence of PBE decreased in the aged oocytes as compared with young oocytes (Figs. S5B and C), which indicates that maternal aging results in meiotic failure in oocytes.

As the orchestration of meiotic progression is highly related to the normal spindle assembly in oocytes [23], we then observed the spindle morphologies and chromosome alignment in the aged oocytes as judged by the staining of α-tubulin. The immunofluorescence results showed that the young oocytes displayed a typical barrel-shaped spindle with well-aligned chromosomes at the equatorial plate (Fig. S6A). By contrast, the aged oocytes exhibited a variety of short, elongated, multipolar or apolar spindles with several scattered or lagging chromosomes (Fig. S6A). Statistically, the rate of aberrant spindles in the aged oocytes significantly increased from 11.8% in the young oocytes to 66.1% (Fig. S6B), especially the short and elongated ones (Fig. S6C). Besides, the percentage of misaligned chromosomes in the aged oocytes remarkably increased as compared with that in the young oocytes by showing the increased width of the chromosome plate at the M I stage (Figs. S6D and E).

The spindle/chromosome abnormalities in the aged oocytes predict the compromised kinetochore-microtubule (K-MT) attachments. To test this, oocytes were exposed to cold treatment to induce the depolymerization of microtubules that were not attached to kinetochores and then immunostained with anti-α-tubulin-FITC antibody to visualize microtubule fibers, with CREST to show kinetochores, and counterstained with Hoechst to observe chromosomes as described previously [23]. We observed a prominently elevated frequency of kinetochores with few cold-stable microtubules in the aged oocytes (Fig. S7A). The quantitative analysis revealed that the number of unattached kinetochores in the aged oocytes was considerably higher than that in the young oocytes (Fig. S7B).

The K-MT attachment errors would inevitably result in the unstable chromosome biorientation, which might contribute to the production of aneuploidy [24]. To determine if this is the case in maternal aged oocytes, karyotypic analysis of M II eggs was performed by chromosome spreading. We observed that most young oocytes had the correct number of univalents to maintain the euploidy (Figs. S8A and B). However, the incidence of aneuploid eggs that had more or less 20 univalents in the aged oocytes increased by more than two-fold as compared with that in the young oocytes (Figs. S8A and B). Collectively, these observations indicate that maternal aging impairs spindle/chromosome structure and thereby evokes the aneuploidy in oocytes.

3.3. Treatment of melatonin in vitro attenuates ROS levels and restores the meiotic defects in aged oocytes

To determine whether supplementation of melatonin can ameliorate the quality of maternally aged oocytes *in vitro* by eliminating the excessive ROS, we treated oocytes with melatonin in an *in vitro* maturation medium for 12 h and then assessed the ROS levels in the aged oocytes. As expected, we found that treatment with melatonin rather than melatonin with luzindole (a preferential melatonin receptor antagonist) substantially reduced the ROS signals as shown by the immunostaining data and the measurement of fluorescence intensity (Fig. 1A and B, Fig. S9). Consistently, the occurrences of DNA damage and apoptosis in the melatonin-treated aged oocytes were also

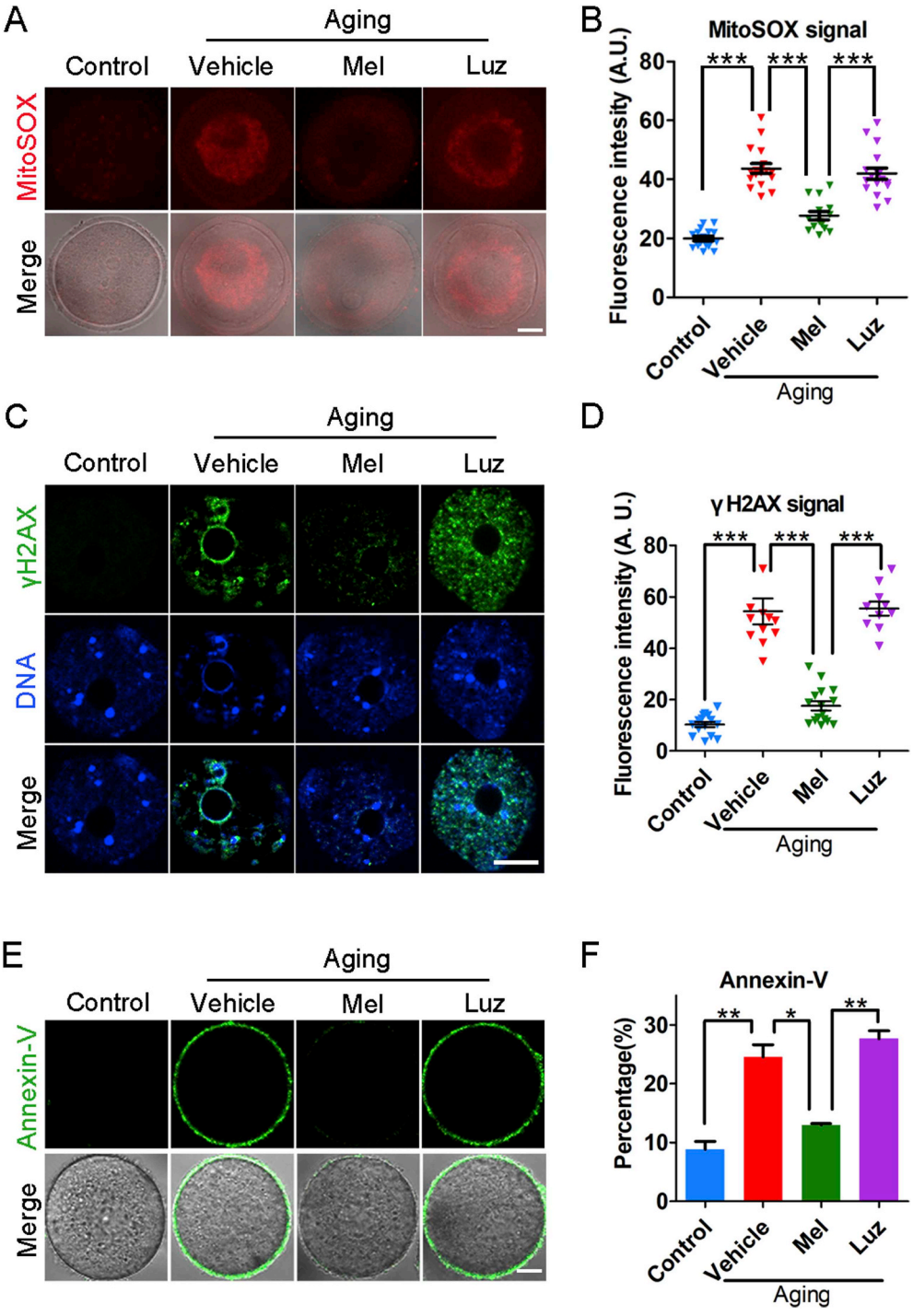

Fig. 1. Effects of melatonin treatment *in vitro* on the ROS levels and apoptosis of aged oocytes. (A) Representative images of ROS levels stained with MitoSOX in young, aged, melatonin-treated and melatonin + luzindole-treated oocytes. Scale bar, 20 μm. (B) Fluorescence intensity of MitoSOX signals was measured in young (n = 16), aged (n = 17), melatonin-treated (n = 14) and melatonin + luzindole-treated (n = 17) oocytes. (C) Representative images of DNA damage stained with γH2AX antibody in young, aged, melatonin-treated and melatonin + luzindole-treated oocytes. Scale bar, 20 μm. (D) Fluorescence intensity of γH2AX signals was recorded in young (n = 15), aged (n = 12), melatonin-treated (n = 16) and melatonin + luzindole-treated (n = 10) oocytes. (E) Representative images of apoptotic status shown by the Annexin-V staining in young, aged, melatonin-treated and melatonin + luzindole-treated oocytes. Scale bar, 20 μm. (F) The rate of early apoptosis was recorded in young (n = 60), aged (n = 57), melatonin-treated (n = 54) and melatonin + luzindole-treated (n = 58) oocytes. Control: young oocytes cultured in M16 medium; Vehicle: aged oocytes cultured in M16 medium; Mel: aged oocytes cultured in M16 medium supplemented with melatonin; Luz: aged oocytes cultured in M16 medium supplemented with melatonin and luzindole. Data were presented as mean percentage (mean ± SEM or SD) of at least three independent experiments. *$P < 0.05$, **$P < 0.01$, ***$P < 0.001$.

significantly decreased as compared with those in the vehicle or luzindole groups (Fig. 1C–F), which suggests that exposure to exogenous melatonin suppresses maternal aging-induced apoptosis.

To further ascertain if meiotic defects could be recovered by reducing ROS levels in melatonin-treated aged oocytes, we next recorded the kinetics of meiotic progression. We observed that melatonin treatment impeded the premature extrusion of the first polar body at 6 and 7 h post-GVBD that occurred in the aged oocytes, although the rate of PBE at 10 h post-GVBD was not altered (Fig. 2A). In addition, the frequency of defective spindles with misaligned chromosomes was remarkably reduced in the melatonin-treated group as compared with the vehicle group (Fig. 2B and C), consequently contributing to the lower incidence of aneuploidy (Fig. 2D and E). As expected, treatment of melatonin with luzindole did not improve the meiotic defects in the aged oocytes (Fig. 2A–E). These results imply that *in vitro* exposure to melatonin is able to, at least partially, reverses the meiotic failure caused by maternal aging.

3.4. Administration of melatonin in vivo eliminates excessive ROS and recovers the meiotic defects in aged oocytes

Since *in vitro* exposure to melatonin could ameliorate the quality of aged oocytes by clearing the high levels of ROS, we next investigated whether administration of melatonin *in vivo* has similar effects. We

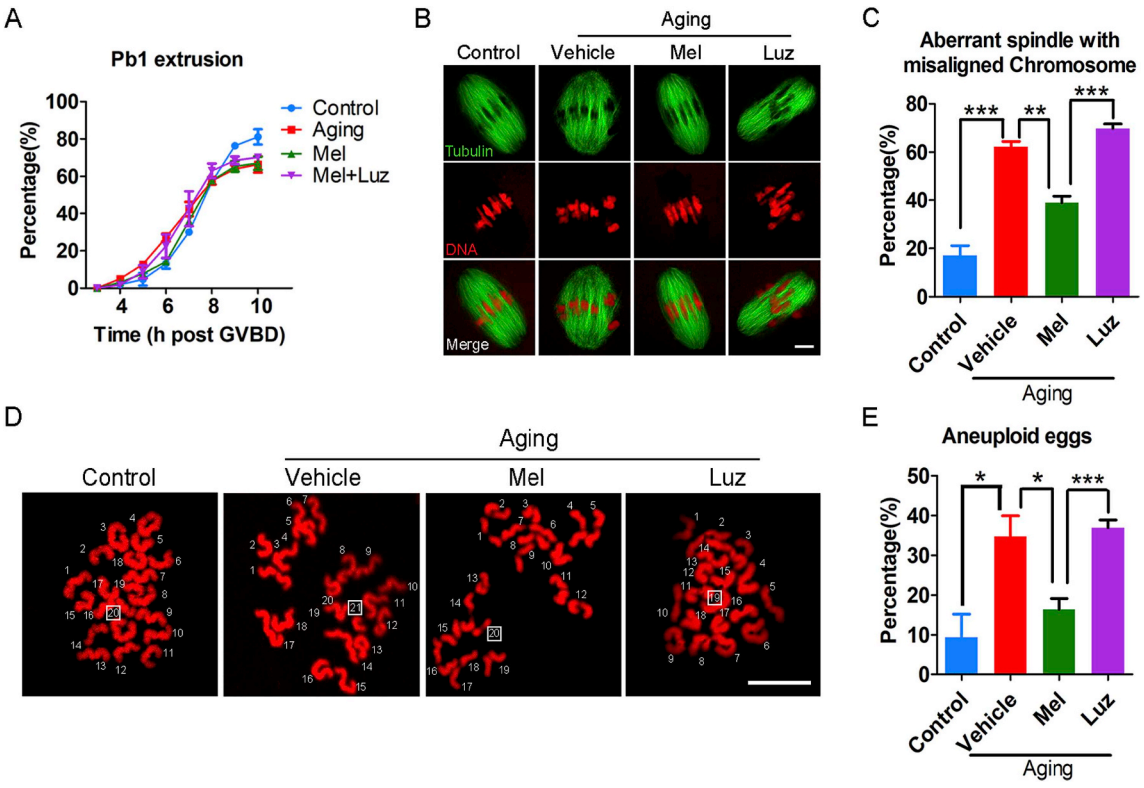

Fig. 2. Effects of melatonin treatment *in vitro* on the meiotic progression, spindle/chromosome structure and euploidy of aged oocytes. (A) The kinetics of PBE was recorded in young (n = 68), aged (n = 58), melatonin-treated (n = 64) and melatonin + luzindole-treated (n = 57) oocytes at consecutive time points of post-GVBD. (B) Representative images of spindle morphologies and chromosome alignment in young, aged, melatonin-treated and melatonin + luzindole-treated oocytes. Scale bar, 3 μm. (C) The rate of aberrant spindle with misaligned chromosome was recorded in young (n = 58), aged (n = 46), melatonin-treated (n = 51) and melatonin + luzindole-treated (n = 43) oocytes. (D) Representative images of euploid and aneuploid MII eggs. Chromosome spreading was performed to count the number of chromosomes in young, aged, melatonin-treated and melatonin + luzindole-treated oocytes. Scale bar, 5 μm. (E) The rate of aneuploid eggs was recorded in young (n = 35), aged (n = 34), melatonin-treated (n = 2) and melatonin + luzindole-treated (n = 27) oocytes. Control: young oocytes cultured in M16 medium; Vehicle: aged oocytes cultured in M16 medium containing ethanol and DMSO; Mel: aged oocytes cultured in M16 medium supplemented with melatonin; Luz: aged oocytes cultured in M16 medium supplemented with melatonin and luzindole. Data were presented as mean percentage (mean ± SEM) of at least three independent experiments. $*P < 0.05$, $**P < 0.01$, $***P < 0.001$.

administered exogenous melatonin for 10 days in age mice and analyzed the melatonin levels in blood serum and follicular fluid. We validated that melatonin levels increased prominently in both blood serum and follicular fluid in the melatonin-administered mice as compared with the vehicle-administered mice (Fig. S10), which indicates that a melatonin-rescued model was successfully established in the aged mice. We then detected ROS levels in the oocytes from melatonin-rescued mice. As expected, the ROS signals were markedly decreased in the oocytes from the aged mice given melatonin rather than with melatonin plus luzindole (Fig. 3A and B, Fig. S11). In agreement with this, the immunostaining and quantification analysis also revealed that the occurrences of DNA damage and apoptosis were significantly declined in the oocytes from the melatonin-rescued mice (Fig. 3C–F).

We further tested whether the reduced ROS levels in the oocytes from the melatonin-administered aged mice would recover the meiotic failure. Consistent with the result from *in vitro* exposure to melatonin, *in vivo* administration of melatonin exhibited similar kinetics of meiotic progression by showing the normal extrusion of the first polar body at 6 and 7 h post-GVBD, but a decreased proportion of PBE at 10 h post-GVBD (Fig. 4A). Likewise, *in vivo* administration of melatonin restored the abnormal spindle/chromosome structure and aneuploidy in the aged oocytes, which was inhibited by the co-administration of luzindole, as evidenced by the immunofluorescence and intensity quantification data (Fig. 4B–E). Altogether, these observations suggest that recovery of melatonin levels in follicular fluid could suppress the excessive ROS-induced DNA damage and apoptosis in maternally aged oocytes, thereby ameliorating the deterioration of oocyte quality.

3.5. Identification of target effectors of melatonin in aged oocytes by transcriptome analysis

To gain insights into the underlying mechanisms regarding how elevation of melatonin levels in follicular fluid improve the oocyte quality in aged mice, we profiled the transcriptomes of GV oocytes derived from young, aged and melatonin-administered mice by RNA sequencing (RNA-seq) to identify the potential target effectors. We found that the transcriptome of the young oocytes was significantly different from that of the aged oocytes by showing that 1731 transcripts were downregulated and 2134 transcripts were upregulated in the aged oocytes (Fig. 5A and B). The same differences were observed in the transcriptome profiles between melatonin-administered and aged oocytes that displayed 1373 downregulated transcripts and 2017 upregulated transcripts in aged oocytes (Fig. 5A, C). In particular, the KEGG enrichment analysis revealed that both differential expressed genes (DEGs) between the young and aged oocytes, or between the melatonin-rescued and aged oocytes in the mitochondrial oxidative phosphorylation and oocyte meiosis pathways were enriched at the top of the list (Fig. 5D and E), consistent with our above-mentioned observations that accumulated ROS and meiotic defects were present in aged oocytes and suppressed in melatonin-rescued oocytes. Expression of several

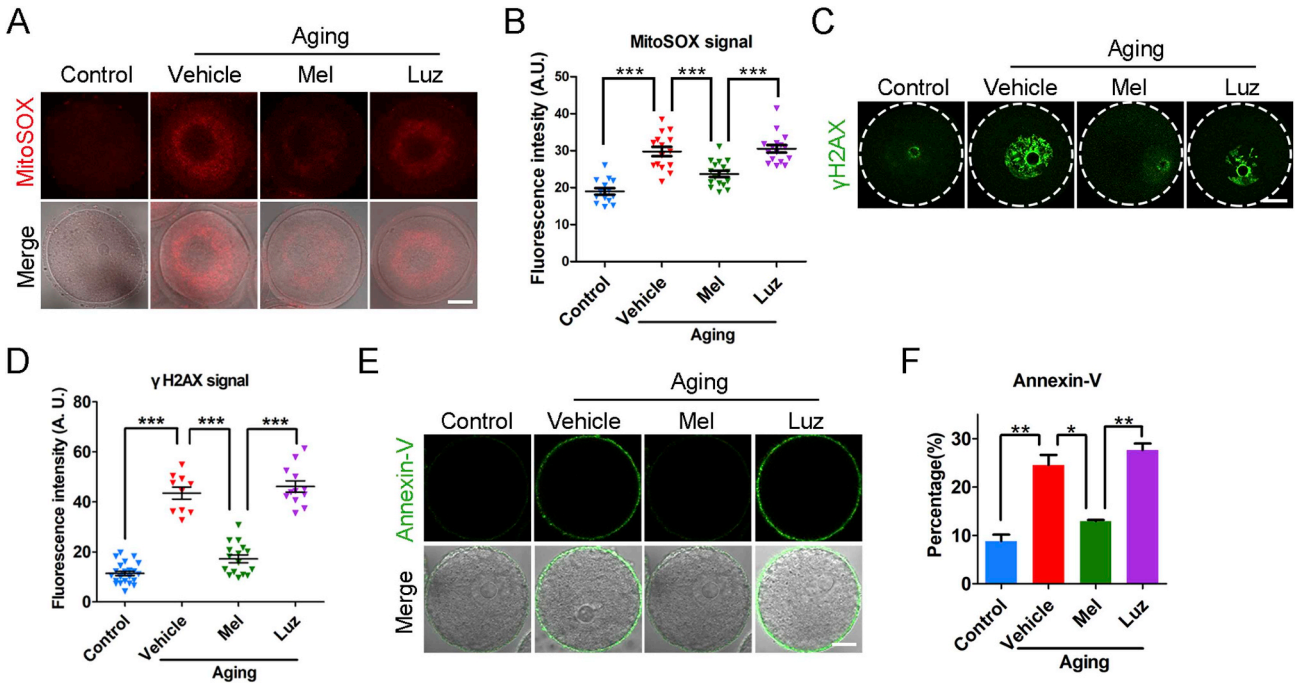

Fig. 3. Effects of melatonin administration *in vivo* on the ROS levels and apoptosis of aged oocytes. (A) Representative images of ROS levels stained with MitoSOX in young, aged, melatonin-administered and melatonin + luzindole-administered oocytes. Scale bar, 20 μm. (B) Fluorescence intensity of MitoSOX signals was recorded in young (n = 14), aged (n = 15), melatonin-administered (n = 17) and melatonin + luzindole-administered (n = 16) oocytes. (C) Representative images of DNA damage stained with γH2AX antibody in young, aged, melatonin-administered and melatonin + luzindole-administered oocytes. Scale bar, 20 μm. (D) Fluorescence intensity of γH2AX signals was recorded in young (n = 23), aged (n = 10), melatonin-administered (n = 16) and melatonin + luzindole-administered (n = 12) oocytes. (E) Representative images of apoptotic status shown by the Annexin-V staining in young, aged, melatonin-administered and melatonin + luzindole-administered oocytes. Scale bar, 20 μm. (F) The rate of early apoptosis was recorded in young (n = 65), aged (n = 42), melatonin-administered (n = 35) and melatonin + luzindole-administered (n = 39) oocytes. Control: oocytes from young mice; Vehicle: oocytes from aged mice administered with PBS; Mel: oocytes from aged mice administered with melatonin; Luz: oocytes from aged mice administered with melatonin and luzindole. Data were presented as mean percentage (mean ± SEM or SD) of at least three independent experiments. $*P < 0.05$, $**P < 0.01$, $***P < 0.001$.

randomly selected transcripts in each group was verified using quantitative real-time PCR (Fig. S12). Among the DEGs, we paid great attention to *Sirt1* because accumulating evidence has validated that the Sirtuin protein family is involved in combatting oxidative stress [25], and *Sirt1* is the only Sirtuin gene present in our transcriptomic data.

3.6. Melatonin eliminates ROS via the Sirt1/Sod2 pathway to improve the quality of maternally aged oocytes

To validate the possibility that the reversed effects of melatonin on oocyte aging is mediated by the activity of Sirt1, we first detected its expression levels by both RT-PCR and immunoblotting analysis, showing that the mRNA and protein levels of Sirt1 were dramatically decreased in the aged oocytes but recovered in the melatonin-rescued oocytes (Fig. 6A, B, C). However, co-administration of melatonin with luzindole did not increase the Sirt1 expression level in the aged oocytes (Fig. 6A, B, C), which implies that the accumulated ROS in the aged oocytes correlates with the reduction of Sirt1.

Mitochondrial Sod2 (superoxide dismutases 2) is thought to be a major antioxidant enzyme scavenging cellular ROS [26] and its activation is regulated by Sirt1 [27]. To test whether the recovery of Sirt1 expression by melatonin would affect the Sod2 expression, we also examined the mRNA and protein levels of Sod2 by using RT-PCR and immunoblotting. The results revealed that the expression trend of Sod2 was highly consistent with that of Sirt1 by showing that Sod2 was substantially reduced in the aged oocytes but restored in the melatonin-administered oocytes (Fig. 6A, B, C). Meanwhile, either inhibition of melatonin by luzindole or inhibition of Sirt1 by EX527 did not recover the protein amount of Sod2 in the aged oocytes (Fig. 6C), which suggests that melatonin administration activates the Sirt1/Sod2 pathway in the maternally aged oocytes.

We next tested whether inhibition of Sirt1 would abolish the elimination of excessive ROS in the aged oocytes by administration of melatonin. The analyses by fluorescence staining and intensity quantification revealed that the ROS signals in the melatonin-administered aged oocytes after EX527 treatment remained at an aged oocyte comparable level (Fig. 6D, E, Fig. S13). Accordingly, the incidence of DNA damage and apoptosis could not be rescued by the melatonin when Sirt1 was inhibited by EX527 (Fig. 6F–I).

We further evaluated the spindle/chromosome structure, and observed that inhibition of Sirt1 did not rescue the spindle assembly and chromosome alignment that was recovered by the melatonin administration (Fig. 7A and B), and thereby did not reverse the high frequency of aneuploidy in the aged oocytes (Fig. 7C and D). Collectively, these observations indicate that activation of the Sirt1/Sod2 pathway by melatonin eliminates the excessive ROS accumulated in the maternally aged oocytes, thus reducing the occurrence of aneuploidy and improving oocyte quality.

4. Discussion

Increasing accumulation of damage via oxidative stress induced by both inborn and environmental factors has been considered as the primary reason that leads to aging [28,29]. Since the discovery of

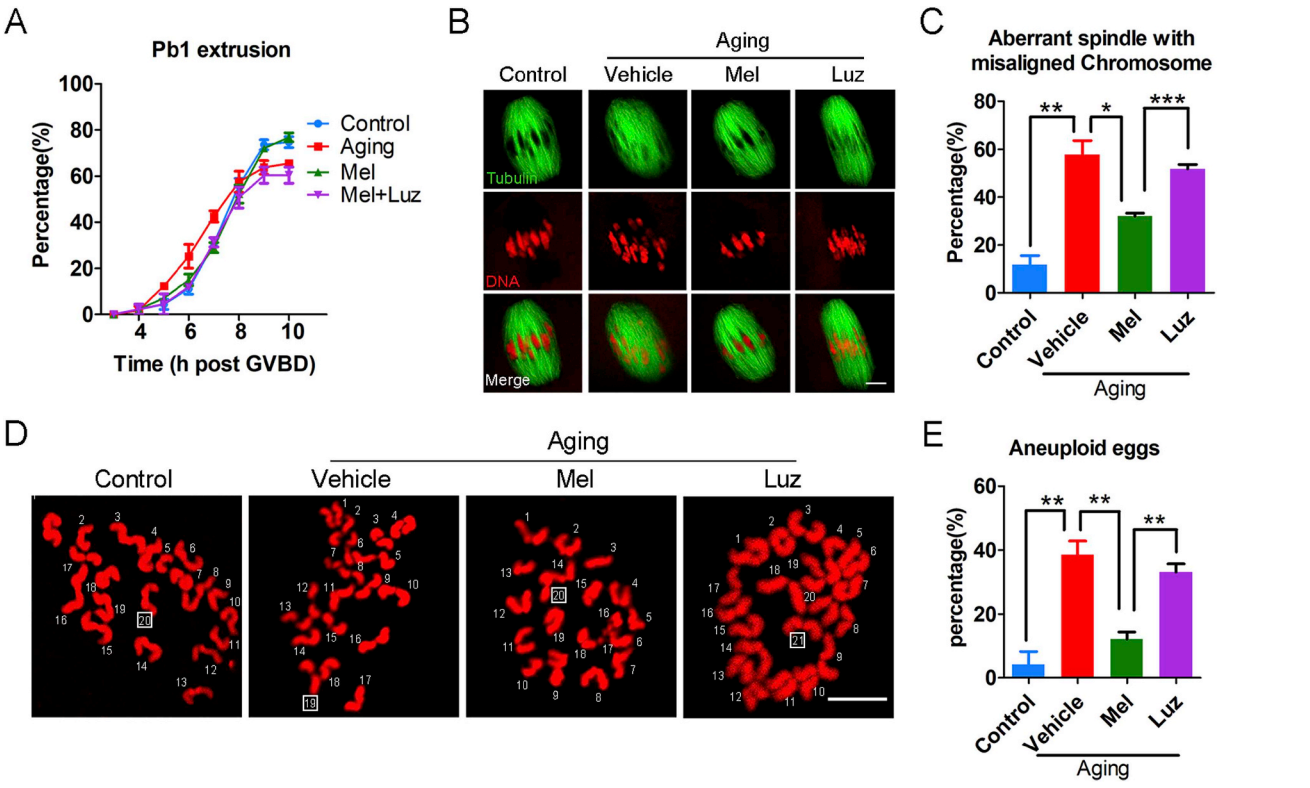

Fig. 4. Effects of melatonin administration *in vivo* on the meiotic progression, spindle/chromosome structure and euploidy of aged oocytes. (A) The kinetics of PBE was recorded in young (n = 61), aged (n = 49), melatonin-administered (n = 56) and melatonin + luzindole-administered (n = 41) oocytes at consecutive time points of post-GVBD. (B) Representative images of spindle morphologies and chromosome alignment in young, aged, melatonin-administered and melatonin + luzindole-administered oocytes. Scale bar, 3 μm. (C) The rate of aberrant spindle with misaligned chromosome was recorded in young (n = 51), aged (n = 40), melatonin-administered (n = 47) and melatonin + luzindole-administered (n = 50) oocytes. (D) Representative images of euploid and aneuploid MII eggs. Chromosome spreading was performed to count the number of chromosomes in young, aged, melatonin-administered and melatonin + luzindole-administered oocytes. Scale bar, 5 μm. (E) The rate of aneuploid eggs was recorded in young (n = 26), aged (n = 24), melatonin-administered (n = 26) and melatonin + luzindole-administered (n = 21) oocytes. Control: oocytes from young mice; Vehicle: oocytes from aged mice administered with PBS; Mel: oocytes from aged mice administered with melatonin; Luz: oocytes from aged mice administered with melatonin and luzindole. Data were presented as mean percentage (mean ± SEM) of at least three independent experiments. $*P < 0.05$, $**P < 0.01$, $***P < 0.001$.

melatonin as a natural antioxidant and its presence in follicular fluid, synthetic melatonin has been applied to assist women in their advanced reproductive ages with poor oocyte quality and low ovarian reserve to increase fertility outcomes [30]. However, the underlying molecular basis and mechanism regarding how melatonin ameliorates declining oocyte quality are still not fully understood. We thus hypothesized that loss of melatonin in follicular fluid during maternal aging would produce an excessive accumulation of ROS and DNA damage, which, in turn, compromises oocyte quality and generates aneuploid eggs.

To confirm this hypothesis, we first detected the melatonin levels in blood serum and follicular fluid. In line with the previous reports that a much higher melatonin level is found in human follicular fluid than in blood serum [18,31], we found an approximately twofold amount of melatonin in follicular fluid than in blood serum from the young mice. We also found that melatonin levels decreased in both blood serum and follicular fluid from the aged mice, which is consistent with the study that showed that the amount of melatonin produced by human pineal gland diminishes with advancing age [32]. Interestingly, our findings revealed that the melatonin levels in follicular fluid reduced more substantially in the aged mice as compared with that in the young mice, which suggests that the maintenance of high melatonin concentration in the follicular fluid microenvironment is crucial for female ovary development and oocyte quality. The decline in melatonin production in many aged individuals may be a primary contributing factor to the low quality of oocytes and ultimately infertility.

Given that the accumulation of oxidative damage might be one of the major contributing factors to the maternal age-related effect of oocytes, we then investigated whether the decline in melatonin level in follicular fluid would cause the production of ROS. In agreement with previous studies [33], we indeed observed an excessive accumulation of ROS in the aged oocytes, accompanied by the existence of positive foci of histone γ-H2AX, which is indicative of DNA damage. This is coincident with the observation that ROS activates ATM to induce H2AX phosphorylation (γ-H2AX) [34]. In addition, oocytes with oxidative stress and excessive DNA damage clearly have a higher ability to activate the intrinsic apoptotic pathway [35]. Our findings also showed the signs of early apoptosis in the aged oocytes.

In accordance with other investigations [24,36–38], we further found that the prominently increased levels ROS and DNA damage inside the aged oocytes impaired the meiotic progression of oocytes by showing the accelerated and decreased extrusion of the first polar body. Particularly, maternal aging led to a higher incidence of spindle assembly defects and chromosome misalignment, accompanied by the incorrect kinetochore-microtubule attachment, thereby resulting in the generation of aneuploid eggs.

To test whether melatonin could recover the meiotic failure of aged

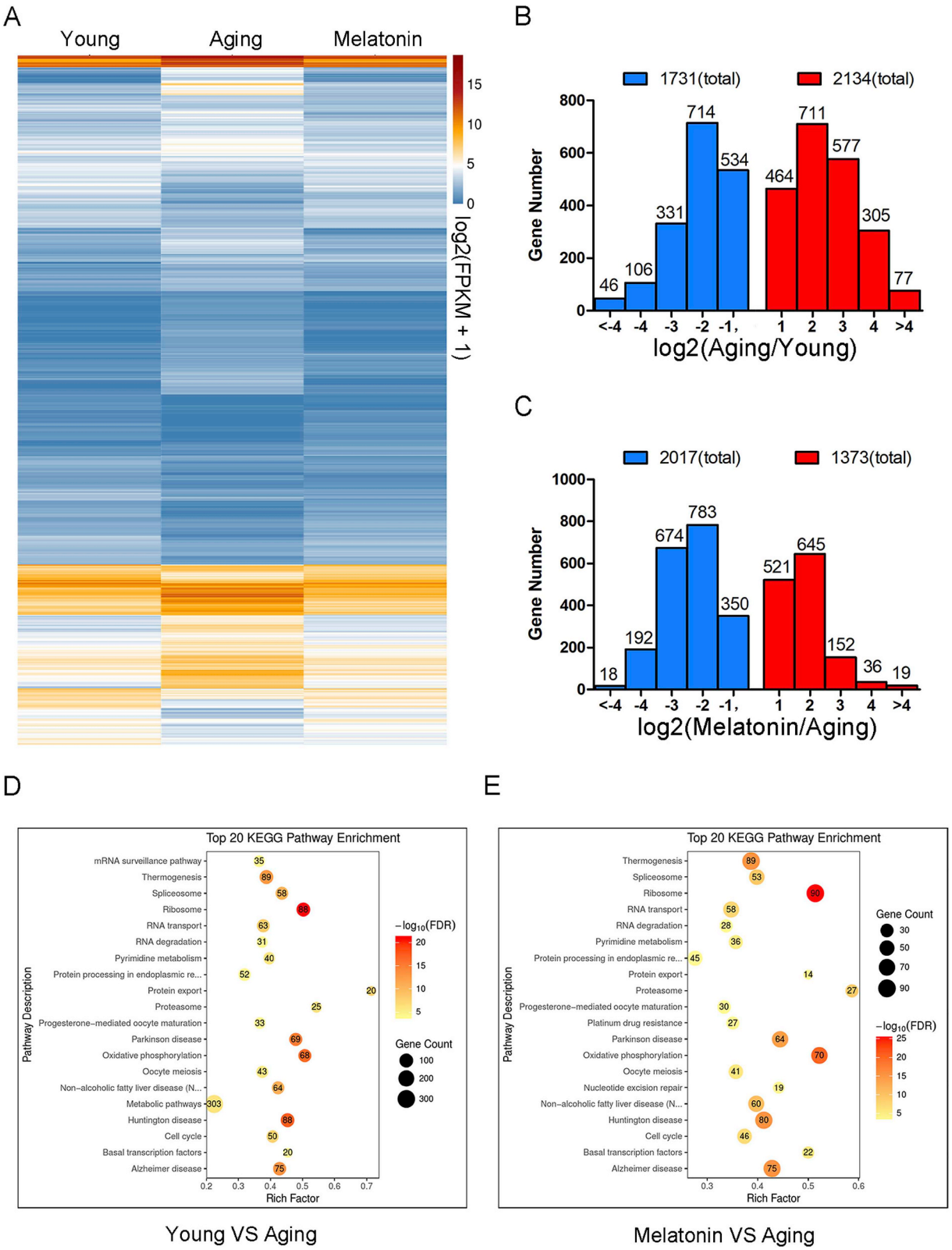

Fig. 5. Effects of melatonin administration *in vivo* on the transcriptome profiling of aged oocytes. (A) Heatmap illustration showing differentially expressed transcripts in oocytes from young, aged and melatonin-rescued mice. (B) Numbers of transcripts that are abnormally repressed (blue) or upregulated (red) in aged oocytes compared to young ones. (C) Numbers of transcripts that are abnormally repressed (blue) or upregulated (red) in melatonin-administered oocytes compared to aged ones. (D) Top 20 KEGG pathway enrichment in young oocytes compared to aged ones. (E) Top 20 KEGG pathway enrichment in melatonin-administered oocytes compared to aged ones. (For interpretation of the references to color in this figure legend, the reader is referred to the Web version of this article.)

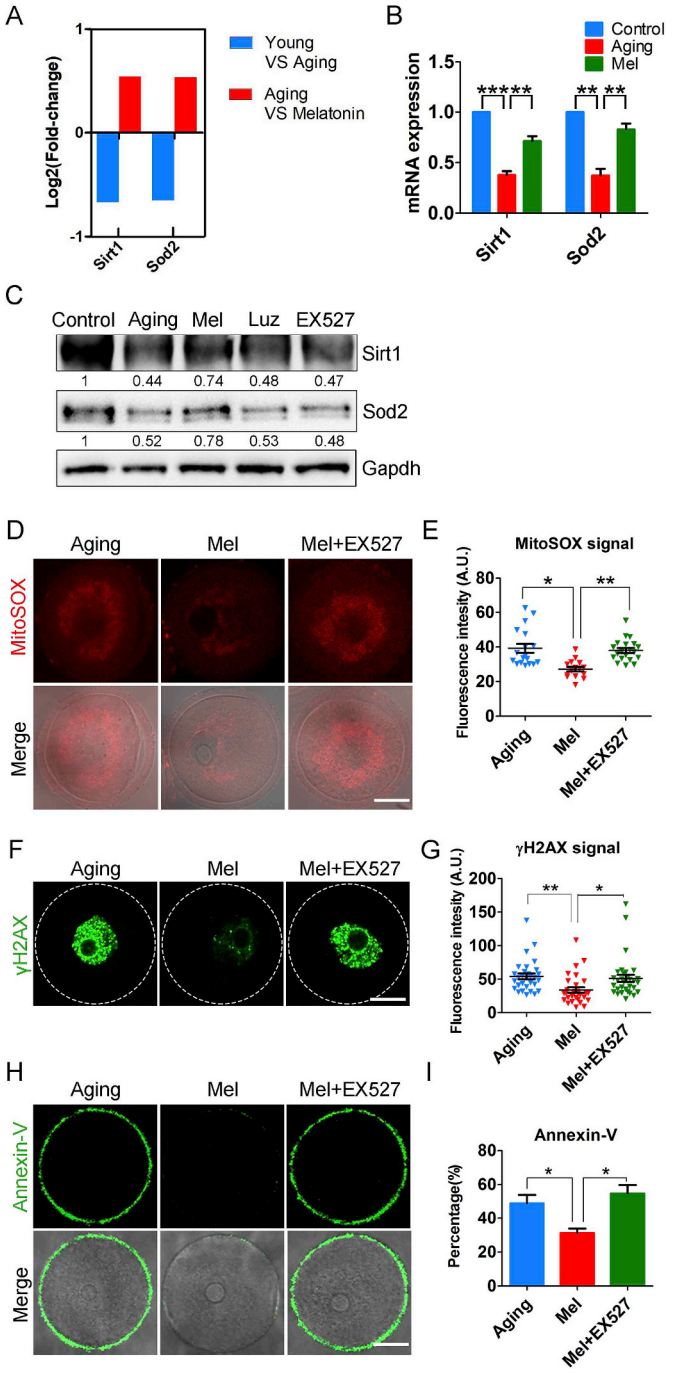

Fig. 6. Inhibition of Sirt1/Sod2 pathway abolishes the melatonin-mediated elimination of excessive ROS. (A) RNA-seq results of *Sirt1* and *Sod2* in young oocytes compared to aged ones (blue), and aged oocytes compared to melatonin- administered ones (red). (B) mRNA expression levels of *Sirt1* and *Sod2* were examined by quantitative RT-PCR in young (blue), aged (red) and melatonin-administered (green) oocytes. (C) Protein expression levels of Sirt1 and Sod2 were detected by immunoblotting in young, aged, melatonin-administered, melatonin + luzindole-administered and melatonin-administered + EX527-treated oocytes. 200 oocytes for each group were collected and immunoblotted for Sirt1, Sod2 and Gapdh. Relative band intensity was calculated using ImageJ software and normalized to Gapdh. (D) Representative images of ROS levels stained with MitoSOX in aged, melatonin-administered and melatonin-administered + EX527-treated oocytes. Scale bar, 20 μm. (E) Fluorescence intensity of MitoSOX signals was recorded in aged (n = 18), melatonin-administered (n = 15) and melatonin-administered + EX527-treated (n = 20) oocytes using the same settings and parameters of the confocal microscope. (F) Representative images of DNA damage stained with γH2AX antibody in aged, melatonin-administered and melatonin-administered + EX527-treated oocytes. Scale bar, 20 μm. (G) Fluorescence intensity of γH2AX signals was recorded in aged (n = 30), melatonin-administered (n = 30) and melatonin-administered + EX527-treated (n = 32) oocytes. (H) Representative images of apoptotic status shown by the Annexin-V staining in aged, melatonin-administered and melatonin-administered + EX527-treated oocytes. Scale bar, 20 μm. (I) The rate of early apoptosis was recorded in aged (n = 37), melatonin-administered (n = 32) and melatonin-administered + EX527-treated (n = 33) oocytes. Control: oocytes from young mice; Aging: oocytes from aged mice administered with PBS; Mel: oocytes from aged mice administered with melatonin; Luz: oocytes from aged mice administered with melatonin and luzindole; Mel + EX527: oocytes from aged mice administered with melatonin were treated by EX527. Data were presented as mean percentage (mean ± SEM or SD) of at least three independent experiments. $^{*}P < 0.05$, $^{**}P < 0.01$, $^{***}P < 0.001$. (For interpretation of the references to color in this figure legend, the reader is referred to the Web version of this article.)

oocytes *in vitro*, we co-incubated GV oocytes with melatonin for some time and then resumed the meiosis in melatonin-free culture medium. We revealed that melatonin treatment effectively attenuated the excessive ROS levels in the aged oocytes. Accordingly, the incidence rates of DNA damage and early apoptosis were also prominently reduced in the melatonin-treated aged oocytes. Additionally, the kinetic analysis of meiotic progression revealed that melatonin treatment rescued the maternal aging-caused acceleration of meiotic progression although the final polar body extrusion was unchanged. Meanwhile, melatonin treatment recovered the impaired spindle assembly and chromosome alignment in the aged oocytes, thereby reducing the frequency of aneuploidy. As expected, treatment with melatonin plus luzindole did not reverse the meiotic defects in the aged oocytes.

To further determine the correlation between melatonin levels in follicular fluid and maternal aging-caused decline of oocyte quality, we administered exogenous melatonin or melatonin with luzindole to aged mice to restore their melatonin levels *in vivo*. We observed that the melatonin levels in both blood serum and follicular fluid were elevated in the young mouse to levels comparable with those in the melatonin group or melatonin with luzindole group, rather than the vehicle group. The increased amount of melatonin in the animals significantly eliminated the accumulated ROS in the aged oocytes, which inhibited the occurrence of DNA damage and apoptosis. More importantly, melatonin administration improved the quality of oocytes from the aged mice by showing the reduced frequency of spindle/chromosome defects and aneuploidy.

Finally, we examined the potential target effectors of melatonin in the aged oocytes. From our transcriptome analysis data, we found that Sirt1 was considerably down-regulated in the aged oocytes but up-regulated in the melatonin-administered oocytes. Increasing evidence has elaborated the interplay between Sirt1 and ROS in both mitotic and meiotic cells via the Sirt1/Sod2 pathway [39,40]. Our data confirmed that increased Sirt1 expression in the melatonin-administered oocytes enhanced the expression of Sod2, thus leading to the reduction of ROS and improvement of oocyte quality. However, these observations could be disrupted by the inhibition of Sirt1 activity, which indicates that Sirt1 indeed mediates the amelioration of aged oocyte quality by melatonin.

Altogether, we provide a body of evidence demonstrating that advanced maternal age-related decline in melatonin level in follicular fluid causes redox perturbation and accumulation of ROS in mouse oocytes, which induces the occurrence of DNA damage and early apoptosis, thereby resulting in meiotic failure and aneuploidy. Particularly, treatment of aged oocytes with exogenous melatonin both *in vitro* and *in vivo* could ameliorate the declining oocyte quality and suppress the generation of aneuploidy via activation of the Sirt1/Sod2 pathway (Fig. S14). Future work should be extended to human oocytes to determine whether this mechanism is conserved between mice and humans, which will elaborate a scientific basis for the application of

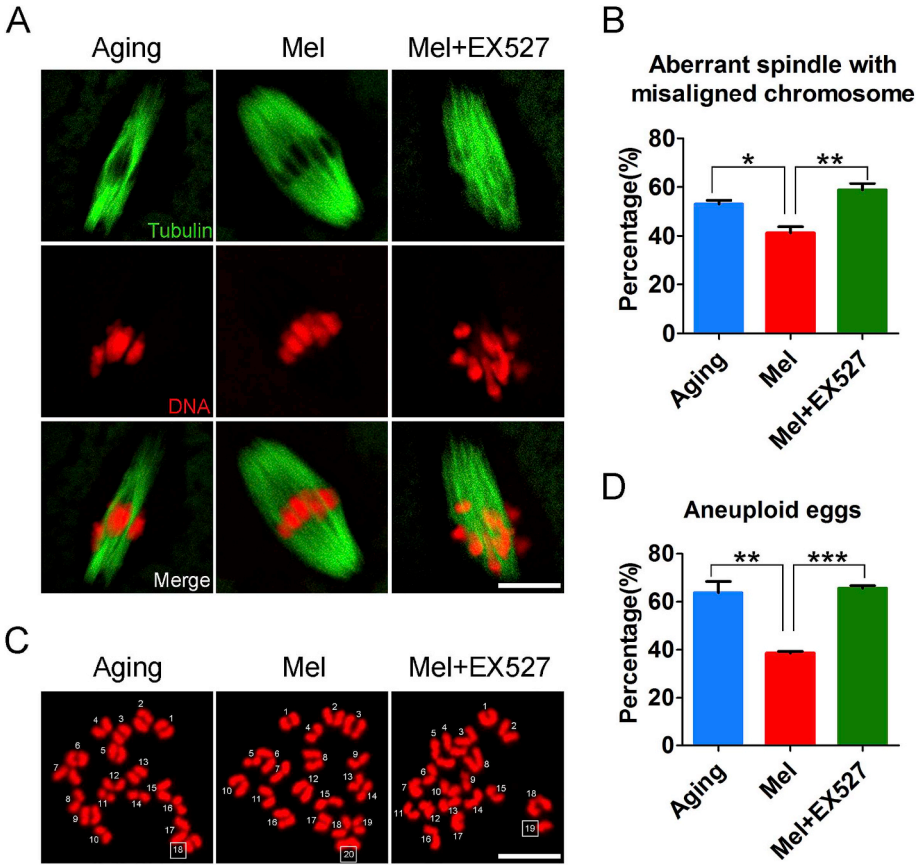

Fig. 7. Inhibition of Sirt1/Sod2 pathway abolishes the melatonin-mediated improvement of aged oocyte quality. (A) Representative images of spindle morphologies and chromosome alignment in aged, melatonin-administered and melatonin-administered + EX527-treated oocytes. Metaphase I oocytes were immunostained with α-tubulin-FITC antibody to display the spindles and counterstained with Hoechst to display the chromosomes. Scale bar, 3 μm. (B) The rate of aberrant spindle with misaligned chromosome was recorded in aged (n = 32), melatonin-administered (n = 39) and melatonin-administered + EX527-treated (n = 34) oocytes. (C) Representative images of euploid and aneuploid MII eggs. Chromosome spreading was performed to count the number of chromosomes in aged, melatonin-administered and melatonin-administered + EX527-treated oocytes. Scale bar, 5 μm. (D) The rate of aneuploid eggs was recorded in aged (n = 30), melatonin-administered (n = 31) and melatonin-administered + EX527-treated (n = 26) oocytes. Aging: oocytes from aged mice administered with PBS; Mel: oocytes from aged mice administered with melatonin; Mel + EX527: oocytes from aged mice administered with melatonin were treated by EX527. Data were presented as mean percentage (mean ± SEM) of at least three independent experiments. $^{*}P < 0.05$, $^{**}P < 0.01$, $^{***}P < 0.001$.

melatonin to improve the quality of oocytes from aged women and the efficiency of assisted reproductive technology.

Conflicts of interest

None declared.

Author contributions

M.Z. and B.X. designed the research; M.Z., Y.L., Y.C. and Y.Z. performed the experiments; M.Z. and B.X. analyzed the data; M.Z. and B.X. wrote the manuscript.

Conflicts of interest

The authors have no conflicts of interest to disclose.

Acknowledgments

This work was supported by the National Key Research and Development Program of China (2018YFC1003802, 2018YFC1004002) and the China Scholarship Council (201806850072).

Appendix A. Supplementary data

Supplementary data to this article can be found online at https://doi.org/10.1016/j.redox.2019.101327.

References

[1] L.C. Kenny, et al., Advanced maternal age and adverse pregnancy outcome: evidence from a large contemporary cohort, PLoS One 8 (2) (2013) p. e56583.
[2] A. Pantazis, S.J. Clark, A parsimonious characterization of change in global age-specific and total fertility rates, PLoS One 13 (1) (2018) p. e0190574.
[3] M.J. Eijkemans, et al., Too old to have children? Lessons from natural fertility populations, Hum. Reprod. 29 (6) (2014) 1304–1312.
[4] T.Y. Tan, et al., Female ageing and reproductive outcome in assisted reproduction cycles, Singap. Med. J. 55 (6) (2014) 305–309.
[5] H.T. Duong, et al., Is maternal parity an independent risk factor for birth defects? Birth Defects Res A Clin Mol Teratol 94 (4) (2012) 230–236.
[6] M.C. Magnus, et al., Role of maternal age and pregnancy history in risk of miscarriage: prospective register based study, BMJ 364 (2019) l869.
[7] L. Ciancimino, et al., Would it be too late? A retrospective case-control analysis to evaluate maternal-fetal outcomes in advanced maternal age, Arch. Gynecol. Obstet. 290 (6) (2014) 1109–1114.
[8] Practice Committee of the American Society for Reproductive, M, Aging and infertility in women, Fertil. Steril. 86 (5 Suppl 1) (2006) S248–S252.
[9] L.J. Heffner, Advanced maternal age–how old is too old? N. Engl. J. Med. 351 (19) (2004) 1927–1929.
[10] F.L. Muller, et al., Trends in oxidative aging theories, Free Radic. Biol. Med. 43 (4) (2007) 477–503.
[11] E. Elmorsy, et al., The role of oxidative stress in antipsychotics induced ovarian toxicity, Toxicol. In Vitro 44 (2017) 190–195.
[12] E.R. Stadtman, Importance of individuality in oxidative stress and aging, Free Radic. Biol. Med. 33 (5) (2002) 597–604.
[13] G.F. Wang, et al., Oxidative stress induces mitotic arrest by inhibiting Aurora A-involved mitotic spindle formation, Free Radic. Biol. Med. 103 (2017) 177–187.
[14] K.M. Holmstrom, T. Finkel, Cellular mechanisms and physiological consequences of redox-dependent signalling, Nat. Rev. Mol. Cell Biol. 15 (6) (2014) 411–421.
[15] J.H. Kim, et al., Melatonin synergistically enhances cisplatin-induced apoptosis via the dephosphorylation of ERK/p90 ribosomal S6 kinase/heat shock protein 27 in SK-OV-3 cells, J. Pineal Res. 52 (2) (2012) 244–252.
[16] B. Malpaux, et al., Melatonin and seasonal reproduction: understanding the neuroendocrine mechanisms using the sheep as a model, Reproduction Suppl. 59 (2002) 167–179.
[17] C. Rodriguez, et al., Regulation of antioxidant enzymes: a significant role for melatonin, J. Pineal Res. 36 (1) (2004) 1–9.
[18] R.J. Reiter, et al., Melatonin and the circadian system: contributions to successful female reproduction, Fertil. Steril. 102 (2) (2014) 321–328.
[19] M. El-Raey, et al., Evidence of melatonin synthesis in the cumulus oocyte complexes and its role in enhancing oocyte maturation in vitro in cattle, Mol. Reprod. Dev. 78 (4) (2011) 250–262.
[20] L.T. Do, et al., Melatonin supplementation during in vitro maturation and development supports the development of porcine embryos, Reprod. Domest. Anim. 50 (6) (2015) 1054–1058.
[21] J. Tong, et al., Melatonin levels in follicular fluid as markers for IVF outcomes and predicting ovarian reserve, Reproduction 153 (4) (2017) 443–451.

[22] D. Wei, et al., Supplementation with low concentrations of melatonin improves nuclear maturation of human oocytes in vitro, J. Assist. Reprod. Genet. 30 (7) (2013) 933–938.
[23] M. Zhang, et al., Stag3 regulates microtubule stability to maintain euploidy during mouse oocyte meiotic maturation, Oncotarget 8 (1) (2017) 1593–1602.
[24] K.T. Jones, S.I. Lane, Molecular causes of aneuploidy in mammalian eggs, Development 140 (18) (2013) 3719–3730.
[25] W. Zhang, et al., Sirt1 inhibits oxidative stress in vascular endothelial cells, Oxid Med Cell Longev 2017 (2017) 7543973.
[26] L. Zhang, et al., Sirt3 prevents maternal obesity-associated oxidative stress and meiotic defects in mouse oocytes, Cell Cycle 14 (18) (2015) 2959–2968.
[27] T. Zhang, et al., SIRT1, 2, 3 protect mouse oocytes from postovulatory aging, Aging 8 (4) (2016) 685–696.
[28] A.T. Perkins, et al., Oxidative stress in oocytes during midprophase induces premature loss of cohesion and chromosome segregation errors, Proc. Natl. Acad. Sci. U. S. A. 113 (44) (2016) E6823–E6830.
[29] H.W. Yang, et al., Detection of reactive oxygen species (ROS) and apoptosis in human fragmented embryos, Hum. Reprod. 13 (4) (1998) 998–1002.
[30] S. Fernando, L. Rombauts, Melatonin: shedding light on infertility?–A review of the recent literature, J. Ovarian Res. 7 (2014) 98.
[31] R.J. Reiter, D.X. Tan, L. Fuentes-Broto, Melatonin: a multitasking molecule, Prog. Brain Res. 181 (2010) 127–151.
[32] D.X. Tan, et al., One molecule, many derivatives: a never-ending interaction of melatonin with reactive oxygen and nitrogen species? J. Pineal Res. 42 (1) (2007) 28–42.
[33] K. Kansaku, et al., Maternal aging affects oocyte resilience to carbonyl cyanide-m-chlorophenylhydrazone -induced mitochondrial dysfunction in cows, PLoS One 12 (11) (2017) p. e0188099.
[34] R. Wan, et al., DNA damage caused by metal nanoparticles: involvement of oxidative stress and activation of ATM, Chem. Res. Toxicol. 25 (7) (2012) 1402–1411.
[35] A. Sanfins, et al., Meiotic spindle morphogenesis in in vivo and in vitro matured mouse oocytes: insights into the relationship between nuclear and cytoplasmic quality, Hum. Reprod. 19 (12) (2004) 2889–2899.
[36] S.I. Nagaoka, T.J. Hassold, P.A. Hunt, Human aneuploidy: mechanisms and new insights into an age-old problem, Nat. Rev. Genet. 13 (7) (2012) 493–504.
[37] S.I. Nagaoka, et al., Oocyte-specific differences in cell-cycle control create an innate susceptibility to meiotic errors, Curr. Biol. 21 (8) (2011) 651–657.
[38] S.I. Lane, Y. Yun, K.T. Jones, Timing of anaphase-promoting complex activation in mouse oocytes is predicted by microtubule-kinetochore sssattachment but not by bivalent alignment or tension, Development 139 (11) (2012) 1947–1955.
[39] Y. Olmos, et al., SirT1 regulation of antioxidant genes is dependent on the formation of a FoxO3a/PGC-1alpha complex, Antioxidants Redox Signal. 19 (13) (2013) 1507–1521.
[40] Q. Yang, et al., Melatonin attenuates postovulatory oocyte dysfunction by regulating SIRT1 expression, Reproduction 156 (1) (2018) 81–92.